

High-Temperature Raman Investigation of Concentrated Sulfuric Acid Mixtures: Measurement of H-Bond ΔH Values between H_3O^+ or H_5O_2^+ and HSO_4^-

G. E. Walrafen,* W.-H. Yang,[†] and Y. C. Chu[‡]

Department of Chemistry, University of Kansas, Lawrence, Kansas 66045-0046

Received: June 18, 2002; In Final Form: August 16, 2002

Forty-two mol percent sulfuric acid is a room-temperature molten salt composed of H-bonded ion pairs $\text{H}_3\text{O}^+ - \text{HSO}_4^-$ (8.2 M) and $\text{H}_5\text{O}_2^+ - \text{HSO}_4^-$ (5.4 M), the former breaking primarily below ~ 360 °C and the latter, mainly between ~ 360 °C and the critical point. These ruptures produce H_2SO_4 and H_2O . Iterative van't Hoff thermodynamic analysis of Raman spectra to 360 °C employing peak height or component area ratios at ~ 905 and ~ 1035 cm^{-1} or at ~ 1165 and ~ 1035 cm^{-1} yielded an average ΔH of 3.2 ± 0.2 kcal/mol corresponding to H-bond breakage between H_3O^+ and HSO_4^- . A Raman ΔH of 5.9 ± 0.3 kcal/mol was measured for the rupture of $\text{H}_5\text{O}_2^+ - \text{HSO}_4^-$ H-bonds between 360 and 513 °C versus ~ 5.7 kcal/mol calculated. H-bonds exist between species other than the two hydronium–bisulfate ion pairs but are not measured by the Raman $\text{H}_2\text{SO}_4/\text{HSO}_4^-$ intensity ratios. Hydrogen bonding wanes near the critical point, ~ 665 °C, at which only neutral species, H_2SO_4 and H_2O (plus some SO_3), remain. A ΔH of 3.5 ± 0.4 kcal/mol was also measured from the 87 mol % acid, close enough to the 3.2 ± 0.2 kcal/mol value to assign both to $\text{H}_3\text{O}^+ - \text{HSO}_4^-$ and also because H_5O_2^+ cannot form in the 87 mol % solution. The integral heat of solution (42 mol %) calculated using Raman data for the two hydronium–bisulfate ion pairs is consistent with the calorimetric value. Values of the dielectric constant were also estimated from Raman data.

Introduction

It has been known for well over 100 years that the negative integral heat of solution of sulfuric acid in water per one total mol of solution displays a maximum below 50 mol % (see Brönsted¹ and references therein). Giauque et al.² reported more recent values of this heat. Treatment of Brönsted's data and Giauque's data with least-squares polynomials^{3,4} yielded identical compositions for the maximum in $-\Delta H$ (42 mol %) but different $-\Delta H_{\text{max}}$ values (Brönsted, 3477.1 and Giauque, 3440.5 cal/mol of solution).⁴

Young et al.⁵ obtained Raman intensity data from sulfuric acid, which we relate to the composition of the maximum heat evolution. They⁵ observed a maximum HSO_4^- concentration of 13.6 M at 25 °C for a composition of 41.7 mol % sulfuric acid, at which the Raman intensities from sulfuric acid molecules and sulfate anions were found to be negligibly small. Young et al.⁵ concluded that a thermodynamic excess of water (i.e., more than one mol of water per mol of acid) is necessary to complete the first dissociation of sulfuric acid.

The results of Young et al.⁵ are connected with those of Brönsted¹ and Giauque et al.² in that the amount of heat evolved per mol of solution is maximal if all of the sulfuric acid molecules react with water to form bisulfate ions and hydronium ions.

The term "hydronium" includes H_5O_2^+ as well as H_3O^+ throughout this work; H_3O^+ or H_5O_2^+ are used in specific cases.

Single-crystal X-ray studies of 50 mol % sulfuric acid provide further support for the results of Young et al., namely, that the solid at -137 °C is composed of HSO_4^- ions H-bonded to H_3O^+ ions.⁶ The X-ray data also indicate short H-bond O–O distances, one as small as 2.54 Å.⁶ This means that the H-bonds are nearly symmetric because the accepted symmetric value is ~ 2.4 Å.⁷

Irish and co-workers⁸ have also reported a high-temperature Raman study of dilute sulfuric acid solutions. This study is important because it highlights the preference of hydronium and sulfate ions to form bisulfate ions and water at elevated temperatures, in direct analogy to the present work, where sulfuric acid molecules and water molecules are preferred over hydronium ions and bisulfate ions at elevated temperatures. See also Klotz et al.⁹

Concentrated sulfuric acid involving a mixture of 7 mols of water and 5 mols of 100% sulfuric acid corresponds accurately to the 41.7 mol % composition studied by Young et al. ($^{5/12} = 0.41666$); hence, the corresponding reaction may be represented by



Because the concentration of bisulfate ion is 13.6 M (ref 5), it is evident from eq 1 that the thermodynamic excess water, needed to drive reaction 1 to completion, corresponds to a concentration of $^{2/5} \times 13.6$ M = 5.4 M at room temperature. (The hyphen in $\text{H}_3\text{O}^+ - \text{HSO}_4^-$ means that this ion pair is hydrogen bonded.) Reaction 1, however, is not mechanistically realistic.

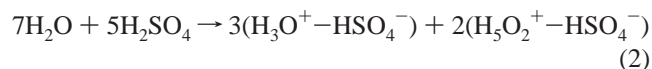
The possibility that water molecules could exist as a separate solution species under the conditions of reaction 1 is nil. Instead,

* Corresponding author. Tel: 785-843-3515. Some of this work was conducted at the Department of Chemistry, Howard University, Washington, D.C.

[†] 701 Stirling Road, Silver Springs, Maryland 20901.

[‡] P.O. Box 68795, Kowloon East Office, Hong Kong, China.

most of the water molecules would be quickly scavenged by H_3O^+ to form H_5O_2^+ (e.g., $[\text{H}_3\text{O}^+-\text{H}_2\text{O}]$). Hence, the mechanistically correct reaction is



It follows that the concentrations of the first and second ion pairs on the right side of eq 2 are 8.2 and 5.4 M, respectively, when the total bisulfate concentration, as determined from Raman data,⁵ is 13.6 M for the 41.7 mol % solution at room temperature. (The room-temperature sulfuric acid molecule and sulfate ion concentrations were found to be negligibly small at 42 mol %; see Young et al.⁵)

The key point to be emphasized here is that Young's thermodynamic driving force that was thought to be the 5.4 M water (eq 1) is actually an ion pair, 5.4 M in concentration, involving the H_5O_2^+ ion. Reaction 1 is forced to the right when H_3O^+ removes the 2 mols of excess H_2O (eq 1) by forming H_5O_2^+ , which then H-bonds with bisulfate ions according to eq 2.

The reactions represented by eq 1 or 2 are reversed by a temperature rise,⁵ just as the bisulfate dissociation reaction studied by Irish et al.⁸ and by Klotz et al.⁹ is reversed by a temperature rise. It seems obvious that the breaking of hydrogen bonds between, for example, H_3O^+ and HSO_4^- , in the 42 mol % acid or between H_3O^+ and SO_4^{2-} in the more dilute acid^{8,9} is the common and overwhelmingly important factor that reverses both the first or second dissociation reactions of sulfuric acid because the acid-base character (i.e., the propensity of a water molecule to accept a proton) should remain about constant.

We took advantage of the high-temperature reversal of the first dissociation of sulfuric acid to obtain Raman spectra from which we were able to extract quantitative ΔH values from peak height and integrated component intensity measurements employing Raman bands centered near 905, 1035, and 1165 cm^{-1} . We then employed an iterative van't Hoff calculation procedure that simultaneously yielded a ΔH value as well as values for the ratios of pairs of peak heights or component intensities of the bisulfate ion in the absence of H_2SO_4 molecules.

The details of our calculation method, as well as of the Raman spectra, are now presented.

Experimental Procedures

Raman spectra were obtained with an Instruments S. A. holographic grating-double monochromator (HG-2S). Scanning and detection were accomplished with the aid of Jobin-Yvon Prism software. Slit widths corresponding to 4 cm^{-1} resolution were used in all cases. Excitation was accomplished with a Coherent argon ion laser at power levels of 600 to 800 mW. All Raman spectra were obtained with the $X(Z,X + Z)Y$ geometry.

The 41.9 mol % sulfuric acid solution was prepared by mixing known masses of 100% sulfuric acid and water, as described in ref 4. The sulfuric acid solution was then placed in a fused-silica Raman sample cell (5 mm i.d.) and frozen by contact with liquid N_2 . The Raman cell containing the frozen acid was evacuated, and its tip was sealed with a torch.

The sealed Raman cell was placed in a closed metal container that was heated electrically in high-temperature measurements. Cooling was accomplished with "blow-off" N_2 in experiments below room temperature. Temperatures were measured with a thermocouple.

Equilibria were established very quickly upon heating to a higher temperature. Nevertheless, some 5 to 10 min were

allowed to elapse before a Raman spectrum was obtained. This provided ample time to achieve consistency in the spectra, for peak positions and widths to reach their equilibrium values.

Quantitative Raman intensity data were obtained (41.9 mol %) from -9 to 360 $^\circ\text{C}$ and also at 513 $^\circ\text{C}$. Intensity data (86.9 mol %) were also obtained from 19 to 326 $^\circ\text{C}$.

Vibrational Assignments for HSO_4^- and H_2SO_4 and Raman Spectra

Vibrational Assignments. The current vibrational assignments treat the OH groups as if they were single atoms, that is, the molecules are treated as "5-atomic". The bisulfate ion has C_{3v} symmetry under this 5-atomic approximation, and the sulfuric acid molecule has C_{2v} symmetry. Moreover, our concern was almost exclusively with the valence vibrations of the bisulfate ion and the sulfuric acid molecule, not with deformation vibrations, S-O-H bending, and torsional vibrations, etc.

We expect four valence vibrations for the bisulfate ion under the 5-atomic approximation. One of these is the totally symmetric stretching of the SO_3 group whose nominal frequency is about 1035 cm^{-1} . The S-(OH) stretch of the bisulfate ion has a nominal frequency of about 905 cm^{-1} . The doubly degenerate asymmetric stretching of the SO_3 group (which makes up the remaining two valence vibrations) has a nominal frequency of roughly 1165 cm^{-1} , but this mode is somewhat weak in the $X(Z,X + Z)Y$ Raman spectrum, and it is relatively very broad.⁴

Four valence vibrations also occur for the sulfuric acid molecule under the 5-atomic approximation. The totally symmetric or in-phase stretching of the two S-(OH) groups occurs near 905 cm^{-1} . This in-phase S-(OH) stretching mode of the sulfuric acid molecule is not resolved from the totally symmetric S-(OH) stretch of the bisulfate ion, but this spectral inseparability is treated mathematically in a subsequent section. The out-of-phase stretching of the two S-(OH) groups occurs in the vicinity of 970 cm^{-1} . The totally symmetric or in-phase stretching of the double-bonded S=O groups occurs in the general vicinity of 1165 cm^{-1} , and it is unresolved from the doubly degenerate stretching of the SO_3 group of the bisulfate ion. This lack of resolution is also treated mathematically in a subsequent section. The fourth valence vibration is the out-of-phase S=O stretching. It is weak and broad in the $X(Z,X + Z)Y$ Raman spectrum and probably refers to the 1350 cm^{-1} feature.

Raman Spectra from the Stretching Region. Raman spectra are shown in Figure 1 for the 41.9 mol % H_2SO_4 solution at temperatures of 360 (upper panel) and -9 $^\circ\text{C}$ (lower panel) and for the valence or SO bond stretching region between 700 and 1500 cm^{-1} .

The -9 $^\circ\text{C}$ spectrum is shown from subsequent thermodynamic analysis to correspond almost exclusively to the bisulfate ion (cf. ref 4). The Raman peak near 905 cm^{-1} arises from S-(OH) stretching. The most intense line at about 1035 cm^{-1} corresponds to the symmetric SO_3 stretching mode, and the weak, broad foot near 1165 cm^{-1} is produced by the doubly degenerate asymmetric stretching motion of the SO_3 group.

The 360 $^\circ\text{C}$ spectrum contains contributions from both the bisulfate ion and the sulfuric acid molecule. However, the peak near 1177 cm^{-1} arises primarily from the in-phase S=O stretching of H_2SO_4 , and the weak, broad shoulder centered near 1350 cm^{-1} may arise from the out-of-phase S=O stretching of H_2SO_4 (see the abrupt fall in intensity near 1425 cm^{-1}). The remaining fundamentals from the sulfuric acid molecule occur near 875 cm^{-1} (in-phase S-(OH) stretching) and near 970 cm^{-1} (out-of-phase S-(OH) stretching that gives rise to the filling-in near 970 cm^{-1} , i.e., between the two most intense peaks).

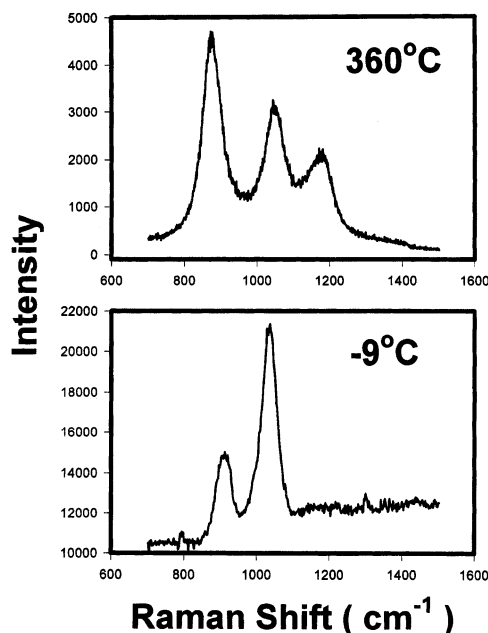


Figure 1. Raman spectra from 42 mol % sulfuric acid at -9 and 360 °C.

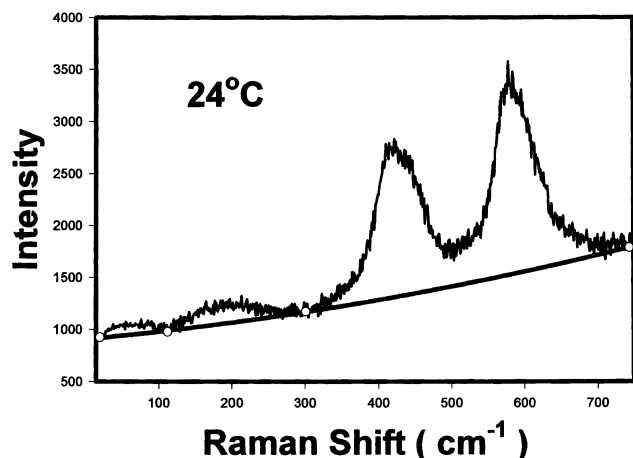


Figure 2. Bose-Einstein-corrected Raman spectrum of 42 mol % sulfuric acid. Note the features above the heavy baseline at 195 and ~ 60 cm^{-1} .

Hydrogen Bonding. A Bose-Einstein-corrected¹⁰ low-frequency Raman spectrum from 41.9 mol % sulfuric acid is shown in Figure 2 for the region from about 20 to 750 cm^{-1} .

The two most intense peaks near 400 and 600 cm^{-1} are deformation modes mainly of the bisulfate ion, but these are not of direct interest here.

The weak, broad peak at 195 ± 10 cm^{-1} is of interest because it relates directly to hydrogen bonding.^{11,12} This feature is an LA phonon peak involved with O–O stretching along the hydrogen bond direction, O–H \cdots O.^{11,12} The very weak ~ 60 - cm^{-1} feature is probably a TA phonon peak associated with hydrogen-bond bending.^{10,11} The TA and LA phonon peaks have both been observed in each of several Bose-Einstein-corrected low-frequency Raman spectra obtained near room temperature, 22 to 24 °C.

The LA phonon peak position of 195 cm^{-1} is roughly 25% higher than that observed for liquid water.^{11,12} This indicates a stronger hydrogen bond between the charged hydronium and bisulfate ions,⁴ where the O–O distance is roughly 2.5 Å⁴ compared to water for which the O–O distance is roughly 2.9 Å and no explicit charges are involved.

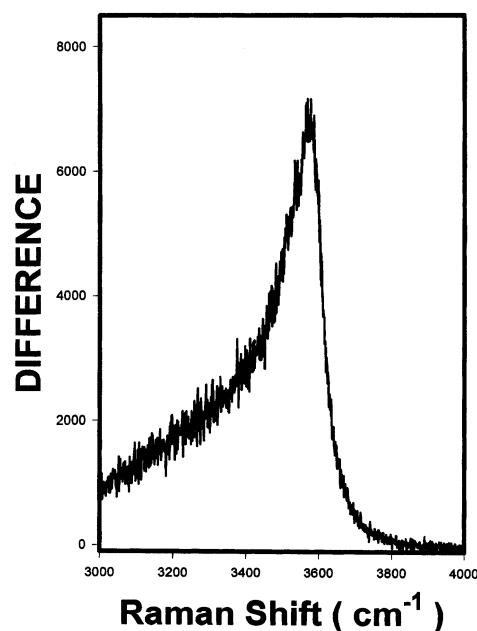


Figure 3. Difference Raman spectrum $350 - 19$ °C in the OH stretching region for 42 mol % sulfuric acid.

An examination of Bose-Einstein-corrected Raman spectra obtained at temperatures of 281 , 316 , and 325 °C indicates that the intensity of the LA phonon feature decreases with temperature rise. The peak also broadens, and its centroid moves downward to roughly 125 to 150 cm^{-1} . These observations indicate that hydrogen bonds are weakened and broken at elevated temperatures (e.g., hydrogen bonds in the ion pair $\text{H}_3\text{O}^+ - \text{HSO}_4^-$, etc).

A Raman difference spectrum from 41.9 mol % sulfuric acid is shown in the OH stretching region in Figure 3. This spectrum resulted from taking the difference between a 350 °C spectrum, which peaks at about 3587 cm^{-1} , and a 19 °C spectrum, which is very broad and peaks near 3475 ± 25 cm^{-1} . The fluorescence background from the 19 and 350 °C spectra was constant. This strong background could be removed by the difference method.

The Figure 3 spectrum arises from the OH stretching vibrations of all of the OH-containing species. However, the room-temperature peak near 3475 cm^{-1} , which is not shown, arises from the combined effects of hydronium ion and bisulfate ion, whereas the high-temperature (e.g., 350 °C) contributions from H_2O and H_2SO_4 become important and are thought to dominate as the critical point is approached.

The OH-stretching difference peak position was found to increase linearly with the temperature rise between about 200 and 360 °C, where it was fit by the least-squares equation $\Delta\nu = 3519.6 + 0.18630t$. Substitution of the critical temperature of the 42 mol % acid, $t = 665$ °C,¹³ into the least-squares equation yields a peak position of 3643 cm^{-1} . This estimated value is in fairly close agreement with the non-hydrogen-bonded OH stretching frequency of liquid water, namely, about 3625 to 3630 cm^{-1} , despite the unusually long extrapolation involved.

H_2O and H_2SO_4 would be expected to be the sole OH-containing species at the critical point. Hence, the rise in the OH-stretching difference peak frequency, and the above frequency agreement, signals the replacement of hydrogen-bonded hydronium bisulfate ion pairs by water and sulfuric acid molecules.

Temperature Dependence of SO-Stretching Peak Frequencies. Peak frequencies versus temperature are shown for

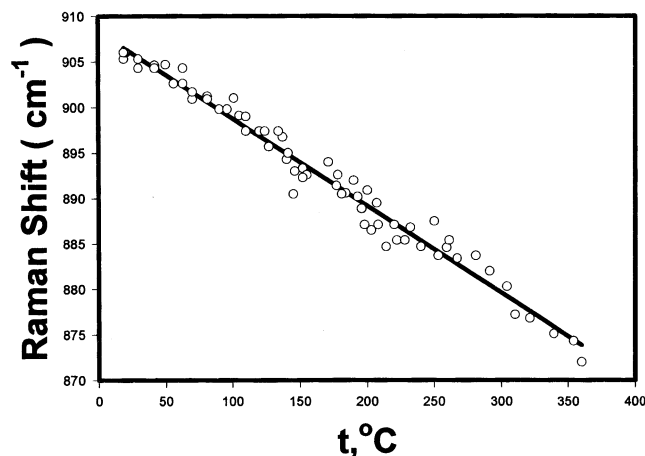


Figure 4. S-(OH) stretching peak frequency versus t , °C for 42 mol % sulfuric acid. The heavy line represents the linear least-squares fit.

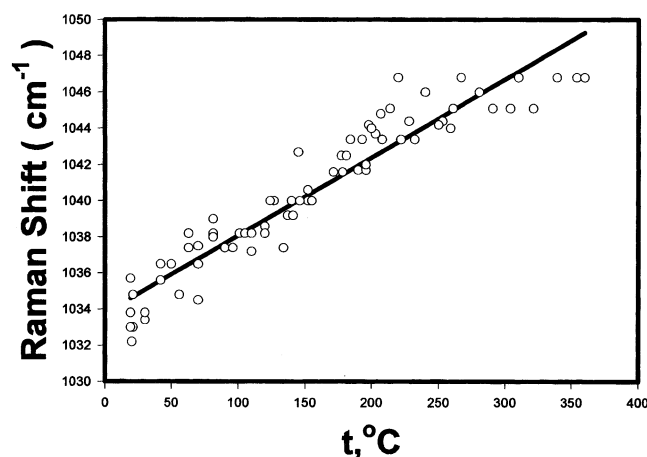


Figure 5. Symmetric SO_3 stretching peak frequency versus t , °C for 42 mol % sulfuric acid. The heavy line represents the linear least-squares fit.

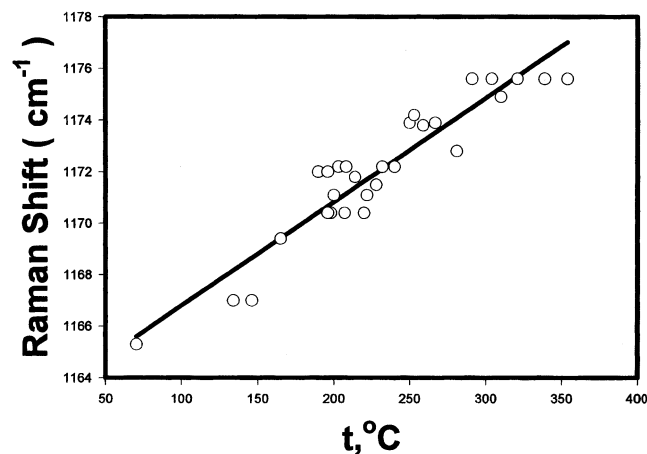


Figure 6. S=O stretching peak frequency versus t , °C for 42 mol % sulfuric acid. The heavy line represents the linear least-squares fit.

the combined bisulfate ion and sulfuric acid molecule symmetric S-(OH) stretching modes in Figure 4, for the symmetric SO_3 stretching mode of the bisulfate ion in Figure 5, and for the combined asymmetric, doubly degenerate bisulfate SO_3 and in-phase S=O stretching modes in Figure 6.

These frequency shifts fall into two classes with temperature rise: (1) a decline for the single-bond S-(OH) modes and (2) a rise for the double-bond S=O modes.

The position of the S-(OH) stretching peak due to the combined modes of the bisulfate ion and the sulfuric acid molecule declines from about 908 cm^{-1} at $0 \text{ }^\circ\text{C}$ to about 874 cm^{-1} at $350 \text{ }^\circ\text{C}$ according to the linear least-squares fit of the data of Figure 4. In contrast, the position of the symmetric SO_3 stretching peak from the bisulfate ion rises from ~ 1038 to $\sim 1053 \text{ cm}^{-1}$ when the temperature increases from 0 to $350 \text{ }^\circ\text{C}$, as seen from the linear least-squares fit of Figure 5. Similarly, the combined (least-squares) position of the asymmetric doubly degenerate stretch of the bisulfate ion and of the in-phase S=O stretch of the sulfuric acid molecule rises from roughly 1163 to $\sim 1177 \text{ cm}^{-1}$ over the $0\text{--}350 \text{ }^\circ\text{C}$ range.

These frequency shifts arise from

(a) the breakage of hydrogen bonds with temperature rise; and

(b) the redistribution of electronic charge within the bisulfate ion and within the sulfuric acid molecule resulting from hydrogen bond breakage. This redistribution produces changes in bond distances and force constants that affect vibrational frequencies.

Breakage of hydrogen bonds, $\text{S-O-H}\cdots\text{O}$, in the case of the S-(OH) stretches of H_2SO_4 and HSO_4^- , allows the proton to lengthen and thus weaken the S-O single bond by pulling electronic charge to itself. This lengthening and weakening of the S-O bond lowers its vibrational frequency (Figure 4). Catti et al.¹⁴ reached the same conclusion using X-ray data from bisulfates. They also found that the S-(OH) distance increases linearly with the rise in the O-O, H-bond distance, in the range of 2.4 to 2.7 \AA .

The doubly bonded S=O groups of H_2SO_4 and HSO_4^- are shortened and strengthened by the loss of hydrogen bonding because the protons of the $\text{H}^+\cdots\text{O}^- - \text{SO}_3\text{H}$ units can no longer abstract so much electronic charge. This yields the frequency rise seen in Figures 5 and 6.

We should also mention that a rise in the symmetric SO_3 stretching frequency has been observed at room temperature for sulfuric acid as the composition rises from ~ 42 to $100 \text{ mol } \%$. This rise occurs because of the increase in the $\text{HSO}_4^- - \text{H}_2\text{SO}_4$ interaction at high mol % compared to the $\text{H}_3\text{O}^+ \cdots \text{HSO}_4^-$ interaction at $42 \text{ mol } \%$. The same effect occurs with the temperature rise at the fixed $42 \text{ mol } \%$ because of the increase in the H_2SO_4 concentration.

General Features of Thermodynamic Analysis. We begin by treating the loss of a proton from H_3O^+ or from H_5O_2^+ , followed by the acceptance of a proton by HSO_4^- , to form H_2SO_4 and H_2O .

We describe this double-well proton-transfer process by



where $\text{P}_{(1)}$ refers to the proton in the hydronium ions and where $\text{P}_{(2)}$ refers to the proton after it has reacted with the bisulfate ion to form H_2SO_4 (i.e., the proton is in the H_2SO_4 molecule). See the subsequent discussion of the forms of various equilibrium constants.

Because the sulfate ion concentration is approaching zero at $\sim 42 \text{ mol } \%$ sulfuric acid and above¹ and because a temperature rise lowers the sulfate ion concentration even further,¹ we invoke charge balance to conclude that $[\text{H}_3\text{O}^+] + [\text{H}_5\text{O}_2^+] = [\text{HSO}_4^-]$. Moreover, because Raman intensity is proportional to concentration,⁵ we write

$$K = \text{P}_{(2)}/\text{P}_{(1)} = [\text{H}_2\text{SO}_4]/([\text{H}_3\text{O}^+] + [\text{H}_5\text{O}_2^+]) = [\text{H}_2\text{SO}_4]/[\text{HSO}_4^-] \propto I_{\text{H}_2\text{SO}_4}/I_{\text{HSO}_4^-} \quad (4)$$

where $I_{\text{HSO}_4^-}$ is the Raman bisulfate ion intensity near 1030–1050 cm^{-1} and $I_{\text{H}_2\text{SO}_4}$ is the intensity due to the sulfuric acid molecule at 905 or 1165 cm^{-1} . These latter two bands result from the combined effects of HSO_4^- and H_2SO_4 .

We treat the 905 cm^{-1} band as an example.

For pure bisulfate ion, that is, in the absence of sulfuric acid molecules, it is evident that $I_{905}/I_{1035} = \text{constant}$, henceforth designated as F . We may thus recast eq 4 by subtracting the 905 cm^{-1} bisulfate ion contribution:

$$K \propto (I_{905} - FI_{1035})/FI_{1035} \quad (5)$$

However, it is convenient to use the letter D for the intensity of any band resulting from the combined effects of the bisulfate ion and sulfuric acid molecule and to use the letter C for the bisulfate ion intensity. This leads to

$$K \propto (D - CF)/CF = (D/CF) - 1 \quad (6)$$

It should be noted that the use of the D/C ratio tends to remove experimental error due to fluctuations in the laser power because the D and C bands are very close to each other.

We next proceed with an iterative van't Hoff treatment involving the equilibrium constant $K \propto [(D/CF) - 1]$.

When the enthalpy change corresponding to an equilibrium is constant, $\ln K = A + B/T$, where $\Delta H = -RB$. Because we are interested solely in the enthalpy change, we may use $[(D/CF) - 1]$ directly instead of K because the unknown proportionality constant will not affect the slope, from which ΔH is determined.

Our procedure was to use the function $T \ln[(D/CF) - 1] = B + AT + ET^2$. An F was then chosen by iteration such that the least-squares fit yielded an E value very close to zero. The initial trial values of F were obtained readily by examining the D/C ratio at the lowest temperatures, where the sulfuric acid molecule concentration goes to zero. Values close to this trial value were employed until the resulting E value was negligibly small, typically about 10^{-8} to 10^{-9} (42 mol %). In this way, we obtained a least-squares fit of the form $\ln[(D/CF) - 1] = A + B/T$ in which A , B , and F were determined simultaneously.

A fit of the raw D/C data then resulted from $D/C = F[\exp(A + B/T) + 1]$.

We demonstrate below that the F value determined from the above least-squares iterative van't Hoff procedure corresponds very closely to the I_{905}/I_{1035} ratio for pure HSO_4^- as it exists in the 42 mol % solution where it is hydrogen bonded (e.g., to H_3O^+). This F value is specific, of course, to the Raman excitation and detection geometry employed, namely, $X(Z,X + Z)Y$, and no polarization scrambler.

We obtained three F values for the 905 to 1035 intensity ratio of bisulfate ion using three different methods to be described below. These values are 0.4164, 0.4150, and 0.4089. An entirely different type of F was obtained for the 1165 to 1035 intensity ratio for bisulfate, namely, 0.08565.

The ΔH values corresponding to the above F values are presented next.

Thermodynamic Results From Intensity Ratios. A. 905- to 1035- cm^{-1} Peak-Height Ratio. Straight baselines were drawn under the Raman contours by averaging through the background noise at 700 and 1500 cm^{-1} (see Figure 1). Peak heights were then determined by averaging through the peak noise and determining the vertical heights above the baselines. It should be noted that the peak positions of the nominal 905- and 1035- cm^{-1} features shifted as indicated in Figures 4 and 5.

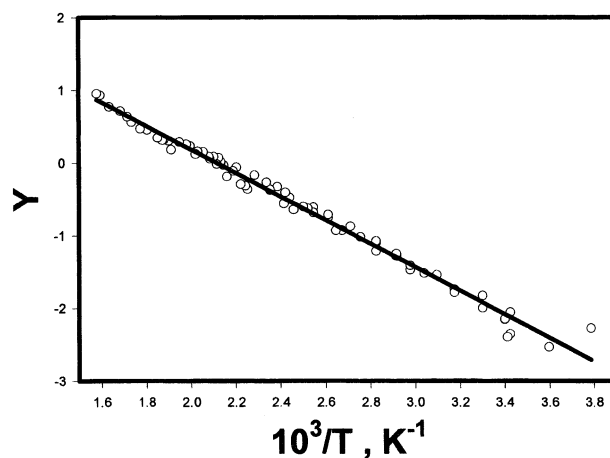


Figure 7. $Y = \ln[(D/CF) - 1]$ versus $1/T$ for 42 mol % sulfuric acid 905/1035- cm^{-1} peak-height ratios. The heavy line represents the least-squares fit; $\Delta H = 3223$ cal/mol.

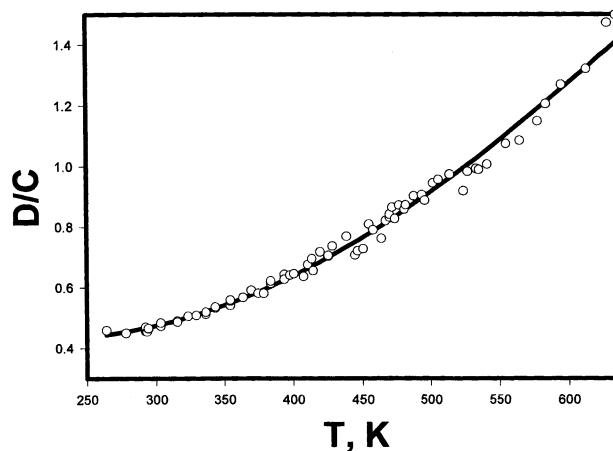


Figure 8. D/C ratio versus T , K for 42 mol % sulfuric acid using Figure 7 data. The heavy-line least-squares fit, $D/C = F[\exp(A + B/T) + 1]$, and A , B , and F parameters are from Figure 7.

Errors in the peak heights due to baseline uncertainty tended to cancel out in the peak-height ratios (i.e., in the D/C values). This cancellation of errors and the ease of determining heights, in contrast to component areas, produced D/C data with an accuracy of about 1–3% at each temperature.

The results of the iterative van't Hoff treatment of the nominal 905- and 1035- cm^{-1} peak-height ratios are shown in Figure 7, where $Y = \ln[(D/CF) - 1]$ is plotted versus $1/T$. The solid line corresponds to the least-squares fit, and its slope corresponds to a ΔH value of 3223 cal/mol with an F value of 0.4164. Error estimates are given subsequently when ΔH values are compared.

The fit of the D/C data is shown in Figure 8. The solid line was calculated from the parameters determined from the least-squares fit of Figure 7 using $D/C = F[\exp(A + B/T) + 1]$.

B. 1165- to 1035- cm^{-1} Peak-Height Ratio. The 1165- to 1035- cm^{-1} peak-height ratios were determined as described in A. A plot of $Y = \ln(D/CF - 1)$ versus $1/T$ is shown for the 1165/1035- cm^{-1} data in Figure 9. The least-squares slope of Figure 9 (solid line) gives a ΔH of 3228 cal/mol with $F = 0.08565$. The agreement with this and the previous value of 3223 cal/mole is excellent. The least-squares fit to the D/C data is shown in Figure 10.

C. Integrated Non-Gaussian-Component Intensity Ratios. Considerable effort was expended in this work to deconvolute the Raman spectral contours (Figure 1) with Gaussian compo-

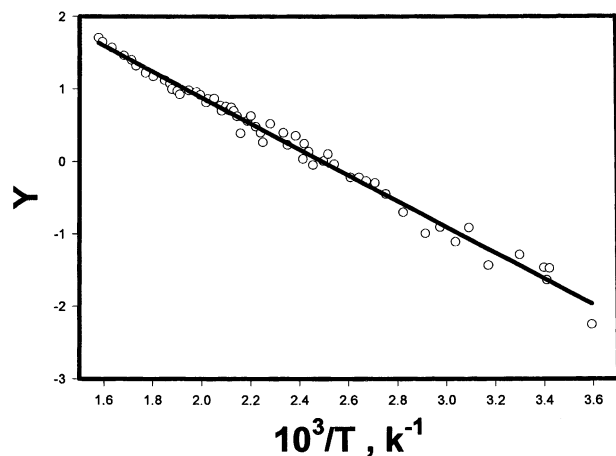


Figure 9. $Y = \ln[(D/CF) - 1]$ versus $1/T$ for 42 mol % sulfuric acid 1165/1035- cm^{-1} peak-height ratios. The heavy line represents the least-squares fit; $\Delta H = 3228$ cal/mol.

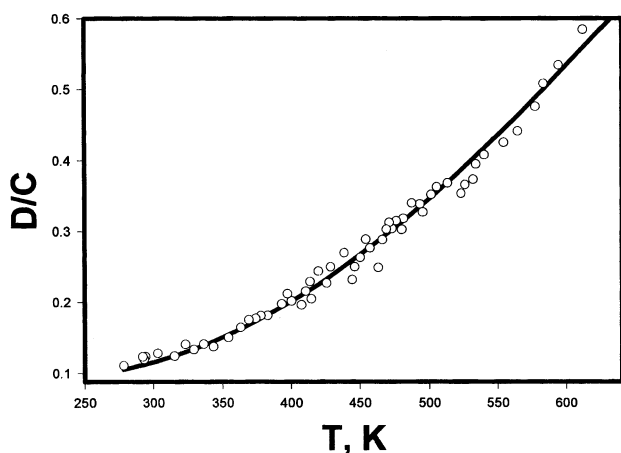


Figure 10. D/C ratio versus T , K for 42 mol % sulfuric acid. The heavy-line least-squares fit, $D/C = F[\exp(A + B/T) + 1]$, and A , B , and F parameters are from Figure 9.

nents. However, it was determined that the component shapes have some non-Gaussian character; the components are a little too sharply peaked, and the base widths are too large to be well fitted by Gaussians. We could, of course, have tried other functions (e.g., Gauss-Lorentz products, etc.), but we used experimentally determined component shapes to avoid criticisms about our shape assumptions.

From an examination of the Raman spectra over the entire temperature range, as well as from our Gaussian deconvolution experiences, we established the fact that the low-frequency "half" of the nominal 905- cm^{-1} feature below the peak did not involve significant contributions from overlap with other components. We therefore proceeded as follows.

The digital data points below the peak of the nominal 905- cm^{-1} feature determined the shape above the peak by symmetry (see Figure 11). These digital points and their mirror image above the peak established the shape function. *The important temperature broadening was thus included for each specific temperature.*

The component shape function was then moved over until its peak coincided with the peak of the nominal 1035- cm^{-1} feature. The shape function was then scaled up or down by a factor, S , until the best fit through the digital intensity data on both the low- and high-frequency sides of the 1035- cm^{-1} peak was obtained (cf. Figure 11). $S = C/D$ (i.e., the reciprocal of the ratio of integrated component intensities D/C used here).

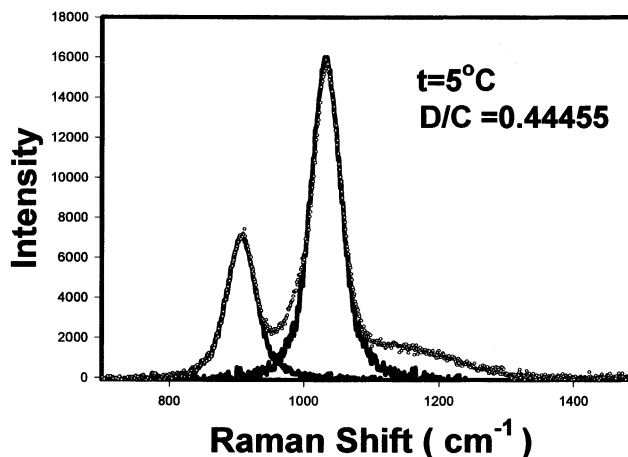
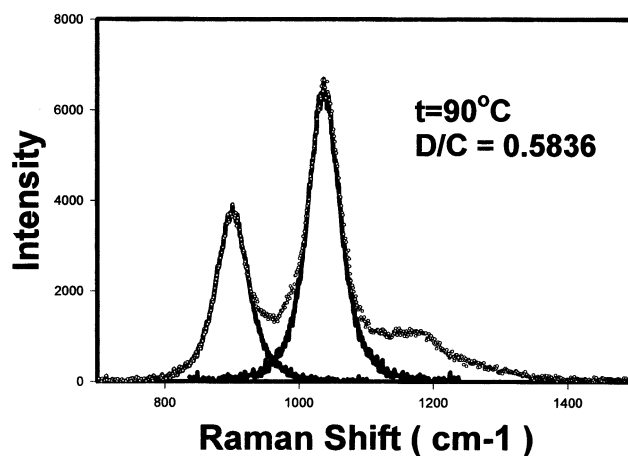


Figure 11. Upper panel, 90 °C. Experimental non-Gaussian components at 905 cm^{-1} (D) and 1035 cm^{-1} (C) determined digitally, represented by heavy curves, for 42 mol % sulfuric acid. The D/C ratio refers to component areas. Lower panel, 5 °C. Note the decline in the D/C ratio with decreasing temperature.

The component shape of the 905- and 1035- cm^{-1} features was the same for a given temperature in this procedure.

This non-Gaussian method was tested at a series of temperatures. We obtained both the 970- cm^{-1} out-of-phase S-(OH) stretching intensity and the nominal 1165- cm^{-1} in-phase S=O stretching intensity of H_2SO_4 by difference. Each was found to rise smoothly with increasing temperature, as required by the increase of the H_2SO_4 molecule concentration.

The non-Gaussian-component intensity ratio data, $\ln[(D/CF) - 1]$ versus $1/T$, are shown in Figure 12. Spectra with the highest signal-to-noise ratios near temperatures corresponding to roughly equal increments of $1/T$ were used. The ΔH from the slope of the solid least-squares line is 3306 cal/mol; the F value is 0.4150. The least-squares fit of the D/C data is shown in Figure 13.

The agreement, $\sim 3\%$, with the previous peak-height results of 3223 and 3228 cal/mol is satisfactory, but the important point is that this method, which does not depend on peak heights, agrees with the two previous methods.

D. Non-Gaussian Intensity Ratios Using Least-Squares Widths. Full widths at half-height (fwhh) and full widths one-third (from the bottom) of the peak height (fwth) are shown for the nominal 905- cm^{-1} S-(OH) mode as a function of temperature in Figure 14(upper and lower panels). These data were fitted with second-degree least-squares polynomials shown by the heavy lines. Full widths at the base of the 905- cm^{-1} feature were also obtained as a function of temperature but are not shown.

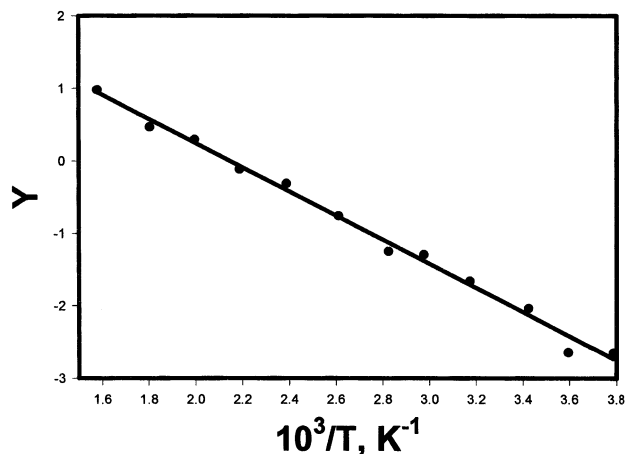


Figure 12. $Y = \ln[(D/CF) - 1]$ versus $1/T$ for 42 mol % sulfuric acid. The heavy line represents the least-squares fit; $\Delta H = 3306$ cal/mol. The $905/1035\text{-cm}^{-1}$ integrated component intensity ratios were determined digitally; see Figure 11.

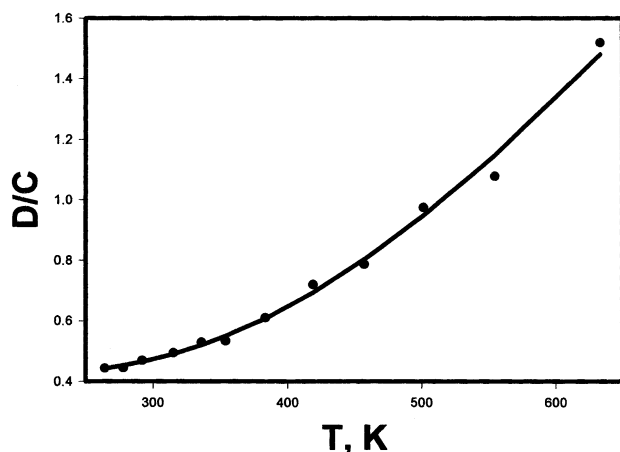


Figure 13. D/C ratio versus T , K for 42 mol % sulfuric acid. The heavy-line least-squares fit, $D/C = F[\exp(A + B/T) + 1]$, and A , B , and F parameters are from Figure 12.

The data of Figure 14 indicate that a limiting width is approached at high temperatures. This limiting width corresponds to extensive hydrogen-bond breakage.

The least-squares fwhh and fwth values were used in conjunction with the full width at the base of the nominal 905-cm^{-1} feature to draw components, by hand, for the nominal 1035-cm^{-1} mode at all temperatures examined here. This procedure also involved averaging through the data near the top of the peak. Smooth, symmetric component shapes were developed by this method. The shape of the 905-cm^{-1} feature was also obtained by the mirror image procedure for all experimental temperatures. This was also accomplished by careful measurements at small frequency increments. The ratio of the integrated component intensities (i.e., I_{905}/I_{1035}) was then determined by weighing the areas. No scaling was involved in this case.

The results of the above procedure are shown in Figure 15 where $\ln[(D/CF) - 1]$ is plotted versus $1/T$. The ΔH corresponding to the least-squares slope shown in Figure 15 (heavy line) is 3062 cal/mol, and the F value is 0.4089 . D/C values are fitted in Figure 16.

The peak-height procedures yielded ΔH values of 3223 and 3228 cal/mol, and the non-Gaussian integrated component intensity ratio methods yielded ΔH values of 3306 and 3062 cal/mol. Although the two latter enthalpy values differ from

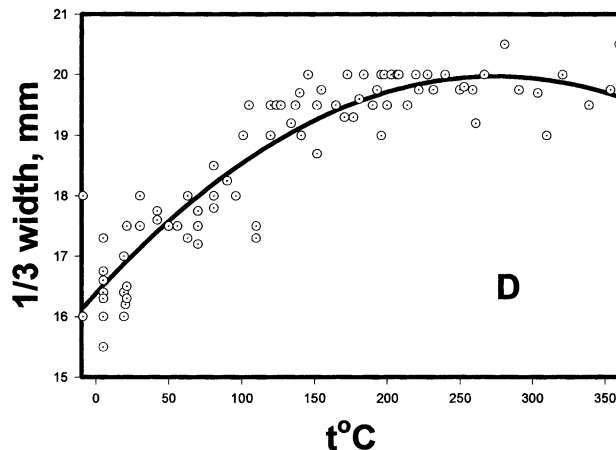
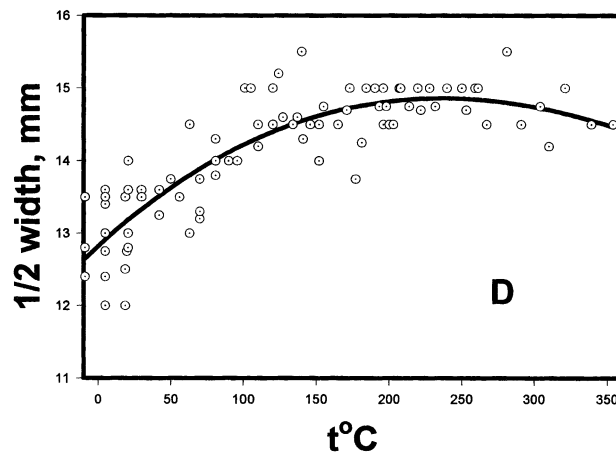


Figure 14. Upper panel: full widths at half-height versus t , $^{\circ}\text{C}$ for the D component, nominally 905 cm^{-1} , for 42 mol % sulfuric acid. Lower panel: full widths at one-third height from the base for the D component. The D component refers to the $\text{S}-(\text{OH})$ stretches of sulfuric acid molecules and bisulfate ions.

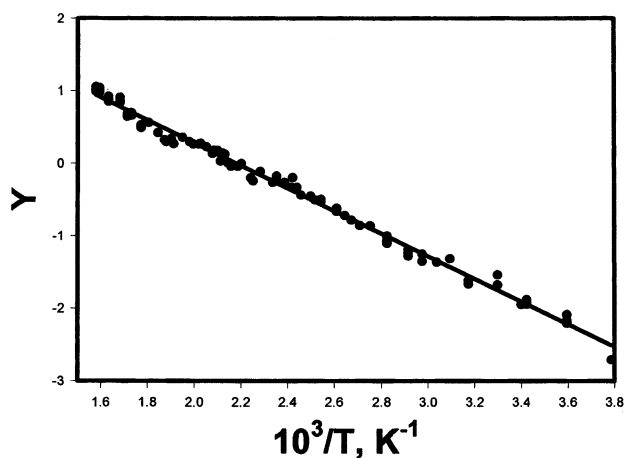


Figure 15. $Y = \ln[(D/CF) - 1]$ versus $1/T$ for 42 mol % sulfuric acid. The heavy line represents the least-squares fit; $\Delta H = 3062$ cal/mol. The $905/1035\text{-cm}^{-1}$ integrated component intensity ratios were determined using the data of Figure 14 plus base widths (not shown).

each other by 8%, their mean is close enough to the peak-height enthalpy values to indicate that no significant difference exists between height and area methods. *Inhomogeneous (temperature) broadening does not vitiate the peak-height ratio method in this specific instance.*

We believe that the most accurate ΔH value may lie within or not far from the 3223 to 3228 cal/mol region. The reason for this is that different peak-height (PH) ratios, $\text{PH}_{905}/\text{PH}_{1030}$

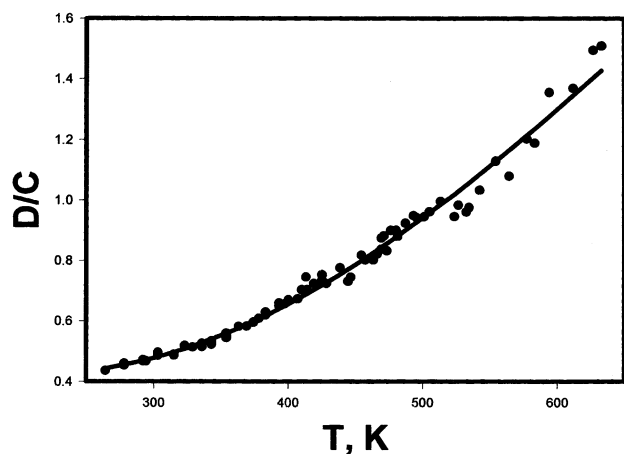


Figure 16. D/C ratio versus T , K for 42 mol % sulfuric acid. The heavy-line least-squares fit, $D/C = F[\exp(A + B/T) + 1]$, and A , B , and F parameters are from Figure 15.

versus $\text{PH}_{1165}/\text{PH}_{1030}$, were employed. Moreover, the peak-height ratios tend to be more precise than component intensity ratios. Nevertheless, objectivity forces us to quote a value of $\Delta H = -3.2 \pm 0.2$ kcal/mol, although the average value of 3225 cal/mol is used subsequently.

We noted that the ΔH values tend to increase with rising F . For example, the ΔH values of 3062 and 3223 cal/mol involve iterative least-squares F values of 0.4089 and 0.4164. We found that increasing F arbitrarily above the iterative least-squares F for the *same* data set increases the least-squares ΔH almost linearly. Also, the iterative least-squares F values are sensitive to the low-temperature D/C ratios, which tend to scatter more than the high-temperature D/C ratios.

It should be noted that four figures are given here for F and that six figures are given subsequently. The number of figures determines how closely the least squares E value comes to zero and is *not* related to significant figures. Note that we quote heats to two significant figures.

Direct measurement of F for the bisulfate ion in dilute sulfuric acid confirms the magnitude of the above F values and is discussed below.

Spectra at Higher Compositions. Raman spectra from 86.9 mol % sulfuric acid were obtained at a series of 30 temperatures between 19 and 326 °C. Spectra corresponding to the highest and lowest temperatures are compared in Figure 17.

Water reacts to completion with sulfuric acid molecules in the 86.9 mol % solution at room temperature.⁴ Hence, H_2O molecules are absent, and 5.634 H_2SO_4 molecules are present per $\text{H}_3\text{O}^+ - \text{HSO}_4^-$ ion pair. This great excess of H_2SO_4 explains why the nominal 905- cm^{-1} feature of Figure 17 is so much more intense relative to the nominal 1030- cm^{-1} feature; compare Figure 17 (19 °C) to Figure 1 (−9 °C).

H_2O_2^+ cannot exist in the 86.9 mol % solution because of the above-mentioned great excess of H_2SO_4 molecules and because H_2O molecules are absent. Hence, a ΔH measured from the I_{905}/I_{1035} Raman intensity ratio must refer solely to the rupture of $\text{H}_3\text{O}^+ - \text{HSO}_4^-$ ion pairs. This rupture produces H_2SO_4 molecules and H_2O molecules as the temperature rises, as described above.

It is known from gas-phase studies that the H_5O_2^+ ion is in a lower energy state than H_3O^+ .¹⁵ Hence, it is logical to conclude that the H_3O^+ ion will break down at a lower temperature than the H_5O_2^+ ion in the acid solution. Nevertheless, the measurement of a ΔH from the 86.9 mol % solution allows for direct assignment of the previous value of 3.2 ± 0.2 kcal/mol to H_3O^+ ,

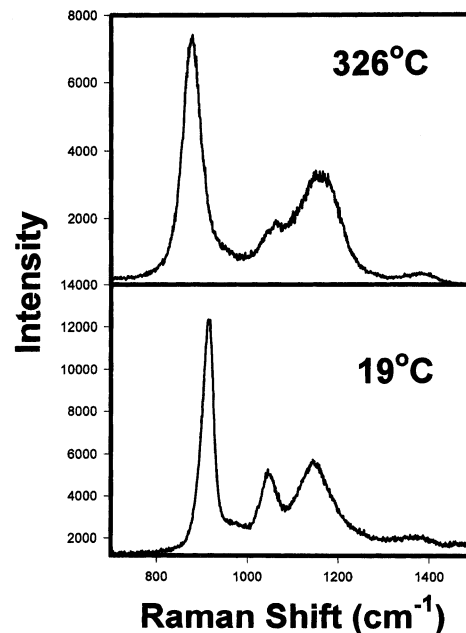


Figure 17. Raman spectra from 86.9 mol % sulfuric acid.

as opposed to a high-temperature value of 5.9 kcal/mol, as shown below.

A ΔH was measured for the 86.9 mol % solution using the I_{905}/I_{1035} Raman intensity ratio, which was determined from non-Gaussian deconvolution described above. However, a new analysis of this ratio is required because the definition of D is different.

For the 86.9 mol % solution, we define $D = I_{905}(\text{H}_2\text{SO}_4, \text{EQ}) + I_{905}(\text{H}_2\text{SO}_4, \text{XS}) + I_{905}(\text{HSO}_4^-)$. (XS = excess, i.e., the 5.634 moles of H_2SO_4 described above, and EQ = H_2SO_4 formed from the rupture of the hydronium–bisulfate ion pair). $C = I_{1035}(\text{HSO}_4^-)$, and F also has its previous definition.

The limiting value of the D/C ratio at very low temperature is no longer F . Instead, this limiting ratio equals $G + F$, where $G = I_{905}(\text{H}_2\text{SO}_4, \text{XS})/I_{1035}(\text{HSO}_4^-)$. We designate $G + F = H$ and then proceed by iterating H in the function $T \ln[(D/C) - H] = B + AT + ET^2$ until E attains a negligibly small value. When ΔH is constant between T_1 and T_2 , we can also write $\Delta H = RT_2T_1/(T_2 - T_1) \ln\{[(D_2/C_2) - H]/[(D_1/C_1) - H]\}$.

Small increments of H are required in the iteration to obtain a negligible E . For $H = 3.46805$, we obtained $E = 5.478 \times 10^{-7}$, which yielded $\Delta H = 3551$ cal/mol. However, we estimate the uncertainty as ± 400 cal/mol, giving a final value of 3.5 ± 0.4 kcal/mol.

The uncertainty is higher for the 86.9 mol % solution than for the 42 mol % solution because the non-Gaussian deconvolution process tends to underestimate the decreasing 1035- cm^{-1} intensity at high temperature when the Raman bands from H_2SO_4 , which occur on either side of the HSO_4^- feature, are increasing and very intense. The $\text{H}_2\text{SO}_4/\text{HSO}_4^-$ concentration ratio starts at the high value of 5.634 at low temperatures and rises further as the temperature increases. Hence, the sulfuric-to-bisulfate concentration ratio becomes too large if the measured Raman HSO_4^- intensity is too low.

The value of 3.5 ± 0.4 kcal/mol is close enough to the value of 3.2 ± 0.2 kcal/mol to assign both to H_3O^+ . But there is no agreement with a value of 5.9 kcal/mol (see next section), which does not change its assignment to H_5O_2^+ .

Measured Raman intensity ratios, D/C , for various temperatures are listed in Table 1 for the 86.9 mol % solution.

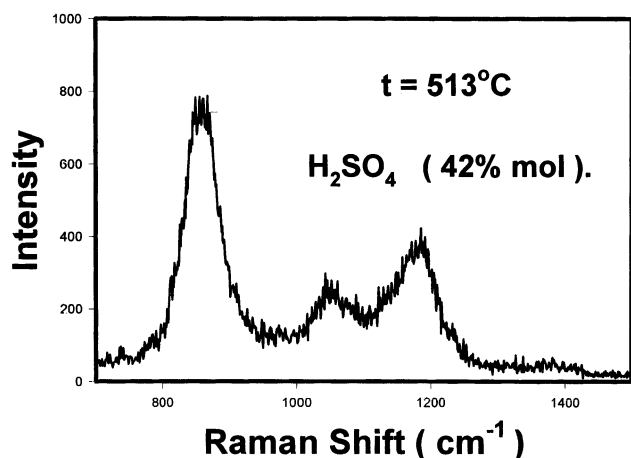


Figure 18. High-temperature Raman spectrum from 42 mol % sulfuric acid.

TABLE 1: D/C Values Versus Temperature for 86.9 mol % Sulfuric Acid

T, K	D/C	T, K	D/C
292.15	3.65	428.15	4.81
295.15	3.67	437.15	4.80
304.15	3.69	443.15	4.82
313.15	3.82	457.15	5.33
338.15	3.83	480.15	5.80
351.15	4.11	500.15	5.94
361.15	4.19	521.15	6.00
376.15	4.01	533.15	6.35
385.15	4.24	547.15	7.10
400.15	4.63	558.15	7.07
417.15	4.60	599.15	7.62

High-Temperature Raman Spectrum from ~42 mol % H_2SO_4 : Determination of ΔH_2 . A Raman spectrum was obtained from ~42 mol % sulfuric acid at 513 °C; see Figure 18. (Tube rupture occurred at 537 °C.)

The weak feature at $\sim 1054\text{ cm}^{-1}$ is produced by the diminished HSO_4^- concentration. The more intense features near 858 and 1186 cm^{-1} result from the relatively larger concentration of H_2SO_4 .

The presence of HSO_4^- necessarily implies the presence of equal concentrations of bisulfate and hydronium ions by virtue of charge balance. Hence, the bisulfate ion concentration and the hydronium ion concentration are lowered by the temperature rise and finally become zero at very high temperatures.

The D/C integrated-component intensity ratio was obtained from repeated non-Gaussian deconvolution of the Figure 18 spectrum; $D/C = 3.15 \pm 0.08$ at 786 K. The D/C ratio measured at 786 K is 49% larger than the D/C ratio obtained by extrapolation according to $\ln[(D/CF) - 1] = A + B/T + ET$.

The calculated ratio ranges from only 2.04 to 2.19 using A , B , E , and F parameters corresponding to Figures 12 and 15. The measured $(D/CF) - 1$ value using F 's from 0.4089 to 0.4150 ranges from 6.59 to 6.70, whereas the extrapolated values are again too small, ranging from 4.00 to 4.28.

The 49% rise in D/C compared to the extrapolated value indicates that a new, additional process occurs at very high temperatures, namely, the disruption of $H_3O_2^+ - HSO_4^-$ ion pairs. We also found that D/C values (e.g., at 360 °C) were beginning to deviate significantly above the extrapolated D/C ratio (e.g., 1.51 measured versus 1.43 extrapolated).

We calculated ΔH_2 using D/C ratios, for example, at 786 and at 633 K; $\Delta H_2 = 5.9 \pm 0.3\text{ kcal/mol}$.

The equilibrium constant must become infinite when the concentration of the reactants goes to zero (i.e., $[HSO_4^-] = 0$),

and thus D/C equals infinity. The equilibrium constant becomes zero at very low temperatures. This may be seen from the fact that $[(D/CF) - 1] = 0$ when $D/C = F$, that is, when only HSO_4^- is present and where $[H_2SO_4] = 0$.

The current plots of $\ln[(D/CF) - 1]$ versus $1/T$ are linear in the region from roughly 5 to 360 °C. A second linear region is also thought to occur from about 360 to 513 °C and above. In addition, enormous positive slopes must occur in $\ln[(D/CF) - 1]$ versus $1/T$ plots at extremely high and at very low temperatures. These enormous slopes refer to the approach to the two singularities involved and do not have physical significance in terms of ΔH values per se.

Critical Point, Equilibrium Constants, and Acidity. A. Critical Point. Hydrogen bonding in 42 mol % sulfuric acid should terminate near, or at, the critical point.¹⁶ Because H-bonding occurs between the waning $H_3O_2^+$ and HSO_4^- ions, we would expect the HSO_4^- concentration to decrease to zero at the critical point and the H_2SO_4/HSO_4^- peak-height (or integrated intensity) ratio, D/C , to diverge and become infinite.

The liquid-to-vapor transformation at T_c almost certainly involves neutral species exclusively.¹⁷ Moreover, hydrogen bonding is very unlikely to be present at 938 K, where $(3/2)RT = 2800\text{ cal/mol}$. We believe that the critical temperature is unusually high because the strong hydrogen bonds between $H_3O_2^+$ and HSO_4^- ions require high temperatures for their complete rupture.

Stuckey and Secoy¹³ reported critical temperatures and densities for aqueous H_2SO_4 solutions between 0 and 100 mol %, although they did not measure critical pressures. T_c is maximal at 61.3 mol % where its value is $\sim 666\text{ °C}$ (939 K). Our (interpolated) value of T_c for the 42 mol % solution is 665 °C (938 K), and we believe that $[HSO_4^-] = 0$ and $K = \infty$ at this unusually high T_c .

Vermeulen¹⁸ has reported total pressures for 42.4 mol % sulfuric acid as well as partial pressures of the vapor species— H_2SO_4 , H_2O , and SO_3 . Most (99.63%) of the total vapor pressure is produced by water at 350 °C. We used the total pressure data to estimate the critical pressure of the vapor. We fit $\ln P_{\text{total}}$ with second- to fifth-degree least-squares polynomials in $(1/T)$. The third-degree polynomial gave the best fit, yielding $P_c = 0.5 \pm 0.1\text{ kbar}$.

SO_3 contributes only 0.0094% to the total vapor pressure at 350 °C. The low SO_3 percentage would appear to agree with the fact that we found no evidence whatsoever for the sharp 1069-cm^{-1} Raman line of SO_3 ¹⁹ in the liquid at 513 °C. However, it is reasonable to expect that SO_3 might appear as the critical point is approached.

B. Equilibrium Constants. $(D - CF)/C$ is directly proportional to the equilibrium constant, K_{EQ} . $K_{EQ} = J_R[(D - CF)/C]$, and $K_{EQ} = J_r F[(D/CF) - 1]$. J_r is the integrated HSO_4^- intensity per mol, nominally at 1035 cm^{-1} , divided by the integrated H_2SO_4 intensity per mol, nominally at 905 cm^{-1} , not including the HSO_4^- contribution. J_R was estimated using integrated component intensity data from 100 and 42 mol % sulfuric acid, where $[H_2SO_4] = 18.62\text{ M}$, and $[HSO_4^-] = 13.6\text{ M}$, respectively. $J_R = 1.69$.

At 50 °C, $K_{EQ} = F[(D/CF) - 1]J_R = 0.4149 \times 0.2064 \times 1.69 = 0.14$, where 0.2064 is the least-squares value of $[(D/CF) - 1]$ (see Figure 12). At 513 °C, $K_{EQ} = 0.4149 \times 6.7 \times 1.69 = 4.7$.

Young et al.⁵ also found the HSO_4^- concentration, as determined from Raman intensities, to decline with the temperature rise between 0 and 50 °C. If we apply our equilibrium constant formulation to Young's concentration data, obtained

from integrated intensities at 50 °C, we obtain a value of 0.1, in satisfactory agreement with our value of 0.14.

An equilibrium constant of 0.14 is fairly large, but the value at 513 °C (786 K) is about 33 times larger. Hence, at the critical temperature of 938 K, we may conclude that reaction 2 has gone entirely to the left, reverting to the reactants H₂SO₄ and H₂O plus some possible decomposition to SO₃.

C. Acidity. Proton transfer occurs because H₂SO₄ is a much stronger acid (proton donor) than H₂O. The stronger acidity of sulfuric acid compared to that of water is obvious from the specific conductance of the 100% acid, which is 103.3×10^{-4} ohm⁻¹ cm⁻¹ compared to that of water, whose specific conductance is only about 55×10^{-9} ohm⁻¹ cm⁻¹ (both at 25 °C). The self-dissociation of pure sulfuric acid produces H₃SO₄⁺, HSO₄⁻, and some HS₂O₇⁻, totalling 0.043 *m*, compared to the total in water, which is only 2×10^{-7} *m*.²⁰

Further evidence in agreement with the above conclusion comes from Raman studies of sulfuric acid over the entire composition range of 0 to 100 mol %. The Raman data demonstrate that H₂SO₄ molecules and H₂O molecules are never present together in measurable quantities as long as the temperature is low (e.g., 25 °C).^{4,5} H₂O molecules make a significant room-temperature contribution only at compositions below those at which the H₂SO₄ concentration is zero.^{4,5}

We suggest that proton transfer from H₂SO₄ to H₂O takes precedence over H-bond formation between the neutral molecules. The H-bond forms *after* the acid–base reaction produces hydronium–bisulfate ion pairs.

Interpretation and Discussion

A. Rationale for the Form of the Equilibrium Constant.

Because of charge balance, it is conventional to use an equilibrium constant of the form $K = [\text{H}_2\text{SO}_4][\text{H}_2\text{O}]/[\text{HSO}_4^-]^2$ for the first dissociation of sulfuric acid. This equilibrium corresponds to H₂SO₄ + H₂O = H₃O⁺ + HSO₄⁻. The inverted form of this *K* was used by Young et al.,⁵ who probably assumed [H₂O] = constant and incorporated it into the equilibrium constant, yielding $K' = [\text{HSO}_4^-]^2/[\text{H}_2\text{SO}_4]$. However, this is unsatisfactory here because [H₂O] is anything but constant, ranging from zero to very large values.

An equilibrium constant without a water term such as $K = [\text{H}_2\text{SO}_4]/[\text{HSO}_4^-]^2$ will vary more rapidly with temperature than the currently used form because of the squared bisulfate term. This stronger temperature dependence leads to a larger ΔH value, ~4.4 kcal/mol; see the van't Hoff plot in the Appendix.

The P₍₁₎ → P₍₂₎ process and its equilibrium constant formulation have several advantages over the above. Laser-power fluctuations tend to be canceled out by use of the [H₂SO₄]/[HSO₄⁻] ratio because the corresponding Raman peaks are separated by only ~130 cm⁻¹. Moreover, errors in the HSO₄⁻ intensity measurement are not squared. In addition, the two environments of the proton correspond to lower and upper energy levels of a double-well potential.

B. Tests of the *F* Parameter. The linearity evident from Figures 7, 9, 12, and 15 and the essential equality of the ΔH values that result are of paramount importance. The validity of this linearity may be determined from tests of the least-squares *F* parameter.

The *F* parameter is the ratio of the intensity (peak height or integrated intensity) of the S–(OH) stretching mode of the HSO₄⁻ ion to the totally symmetric SO₃ stretching mode. Hence, the *F* parameter is fixed, although it can vary slightly because of experimental uncertainty. (A second type of *F* parameter, described above, is fixed at a different value.)

TABLE 2: Iterative, Least-Squares Parameters for 42 mol % Acid^a

<i>B</i>	<i>A</i>	<i>E</i>	<i>F</i>	ΔH^*	method
−1622	3.430	1.244/10 ⁹	0.4164	3223	905/1035 PH
−1624	4.364	2.111/10 ⁹	0.08565	3228	1165/1035 PH
−1664	3.571	−9.141/10 ⁸	0.4150	3306	905/1035 area
−1541	3.346	8.167/10 ⁹	0.4089	3062	905/1035 area

^a Units are cal/mol. $\Delta H = -1.9873B$.

TABLE 3: Measured *F* Values (905/1035 cm⁻¹)

	42 mol %	7.2 mol %
	−9 °C	room temperature
height	0.412 ± 0.01	area 0.410 ± 0.005
area	0.44	
computer	(single measurement)	
area	0.426 ± 0.01	
by hand		

Two evaluations of the constancy of the *F* parameter are presented in Tables 2 and 3.

Three comparable *F* values in Table 2 are 0.4164, 0.4150, and 0.4089, averaging 0.4134. We estimate that the experimental error involved in measuring a single *F* value (e.g., at low temperature) can be as large as 7%. The least-squares *F* deviations of Table 2, 0.5 to 1.0%, fall well below this 7% error estimate.

The corresponding ΔH values of Table 2 are 3223, 3306, and 3062 cal/mol, averaging, 3197 cal/mol. These three experimentally constant ΔH values correspond to the *F* constant to within 1% despite the fact that three different methods—peak-height ratio, Figure 7; computer-integrated intensity ratio, Figure 12; and hand-determined (component width) integrated intensity ratio, Figure 15—were involved.

The concentration of H₂SO₄ declines with decreasing temperature at 42 mol % and should approach zero at a very low temperature.

This means that the *D/C* ratio approaches and finally reaches the true value of *F* as temperature declines. *F* values measured for the 42 mol % solution at −9 °C are presented in Table 3. These values are 0.412 ± 0.01, 0.44, and 0.426 ± 0.01. The agreement with the average of three iterative least-squares *F* values, 0.4134, is within experimental error (0.3%), averaged over several measurements (to 6%) for a single measurement.

A value of *F* involving a different type of measurement is also presented in Table 3. This involves a low acid composition, 7.2 mol %, for which H₂SO₄ molecules are absent but SO₄²⁻ ions are present.^{4,5} In this case, the intense, polarized, symmetric stretching mode of the sulfate ion at 981 cm⁻¹ falls midway between the two modes of the bisulfate ion at 1048 and 898 cm⁻¹.

Non-Gaussian deconvolution of the Raman spectrum from the 7.2 mol % acid solution was accomplished. This yielded the ratio, *F*, of the integrated HSO₄⁻ intensities centered at 898 and 1048 cm⁻¹. The average *F* value, from several deconvolutions, is 0.410 ± 0.005, in good agreement (1%) with the average least-squares iterative *F* value.

We regard the above agreement to be especially significant because it involves an entirely different acid composition. Also, the ratio of 0.410 ± 0.005 could be measured correctly at room temperature because H₂SO₄ molecules do not exist in the 7.2 mol % solution.^{4,5}

A fourth ΔH value of 3228 cal/mol, obtained from peak-height ratios, is presented in Table 2. This value is important because it agrees with the three other values in the Table despite the fact that it involved the 1165-cm⁻¹ feature as opposed to

the 905-cm⁻¹ component. The agreement with the ΔH value from the 905/1035-cm⁻¹ peak-height ratio is especially close, 0.2%.

The A values of Table 2 are proportional to the entropy change. The A values are experimentally constant for the 905/1035-cm⁻¹ component ratios, averaging 3.449. This constancy constitutes a further test of the iterative method. The A value for the 1165/1035-cm⁻¹ ratio is different because it involves a different ratio of molar intensities; it should not agree with the three other values, although the entropy change is the same.

The E values of Table 2 were made to be as close to zero as possible by the iteration of F . These E values relate to the curvature of the $\ln[(D/CF) - 1]$ versus $1/T$ plot, as seen from $[(\partial Y/\partial(1/T))_P = B - ET^2]$, where $Y = \ln[(D/CF) - 1] = A + B/T + ET$. A positive E value, in three of the four cases, corresponds to upward concavity, whereas a negative E value, resulting in one case, corresponds to downward concavity. Such small positive and negative curvatures are not significant within the scatter of the data and relate only to negligible E values.

C. Analysis of the Integral Heat of Mixing at 42 mol %.

We use a basis of 1 mol of HSO₄⁻. The heat of forming 1 mol of HSO₄⁻ in 42 mol % sulfuric acid is -3477.1 cal/0.42 mol = -8278.8 cal/mol Brønsted^{1,3} versus -8191.7 cal/mol Giauque^{2,3,4}. We know that 8191.7 cal/mol should rupture 0.381 mol of H₅O₂⁺-HSO₄⁻ and 0.619 mol of H₃O⁺-HSO₄⁻, forming H₂SO₄ and H₂O molecules. Hence, $0.619F_1\Delta H_1 + 0.381F_2\Delta H_2 = 8191.7$ cal/mol. $\Delta H_1 = 3.2 \pm 0.2$ kcal/mol, ΔH_2 is $\sim 5.9 \pm 0.3$ kcal/mol, F_1 is a factor related to H₃O⁺-HSO₄⁻, and F_2 is a factor related to H₅O₂⁺-HSO₄⁻. F_1 and F_2 are calculated and discussed below.

F_1 and F_2 were calculated from simultaneous equations for compositions of 40 and 42 mol %. We first used $0.5F_1(3225) + 0.5F_2(5900) = 8580.7$ for 40 mol % and $0.61905F_1(3225) + 0.38095F_2(5900) = 8191.7$ for 42 mol %. The simultaneous solution gives $F_1 = 2.154$ and $F_2 = 1.731$ when $\Delta H_1 = 3225$ cal/mol and $\Delta H_2 = 5900$ cal/mol.

Values of F_1 and F_2 that are close to those from simultaneous equations may be obtained from $F_1\Delta H_1 = \Delta H_1 + (n/2)\Delta H_{HB}$ and $F_2\Delta H_2 = \Delta H_2 + (m/2)\Delta H_{HB}$, where $\Delta H_{HB} = 2430$ cal/mol.²³ When $\Delta H_1 = 3225$ cal/mol and $\Delta H_2 = 5900$ cal/mol and when $n = 3$ and $m = 4$, we obtain $F_1 = 2.131$ and $F_2 = 1.824$. n is the number of H-bonds shared between H₃O⁺-HSO₄⁻ and its nearest neighbors, and m is the corresponding number for H₅O₂⁺-HSO₄⁻.

The agreement, 2.154 and 1.731 versus 2.131 and 1.824, is good enough to indicate that the function of the F_1 and F_2 values is to include the H-bond energies *not* measured by the Raman sulfuric/bisulfate intensity ratios. Only the explicitly charged H-bonds between the hydronium and the bisulfate ions are measured by the current Raman method, but all pertinent energies must be included in calculating the integral heat of solution.

From the relations $F_1 = (\Delta H_1 + 3645)/\Delta H_1$ and $F_2 = (\Delta H_2 + 4862)/\Delta H_2$ and $0.61905F_1\Delta H_1 + 0.38095F_2\Delta H_2 = 8191.7$, it is easy to show that $0.61905\Delta H_1 + 0.38095\Delta H_2 = 4083.1$. Note that the current Raman method measures only about 4083/8192 or one-half of the total heat.

We next used combinations of ΔH_1 values in the range of 3062 to 3306 cal/mol (Table 2) and ΔH_2 values in the uncertainty range of 5600 to 6200 cal/mol in the preceding equation and compared the result to 4083.1. The lowest value of $\Delta H_1 = 3062$ cal/mol plus $\Delta H_2 = 5742$ cal/mol yielded 4083, and the lowest value of $\Delta H_2 = 5600$ cal/mol plus $\Delta H_1 = 3150$

cal/mol yielded 4083. Hence, $\Delta H_1 \approx 3100$ cal/mol, and $\Delta H_2 \approx 5700$ cal/mol (giving 4090).

The conclusion from the above calculations is that the experimental values of $\Delta H_1 = 3.2 \pm 0.2$ kcal/mol and $\Delta H_2 = 5.9 \pm 0.3$ kcal/mol are consistent with the integral heat of solution measured calorimetrically.

D. Dielectric Constant of 42 mol % Sulfuric Acid. The dielectric constant has not been measured, to our knowledge, for a 42 mol % sulfuric acid solution,²⁴ undoubtedly because of problems involving high electrical conductivity. Moreover, if the dielectric constant could be measured, one might expect the corresponding microscopic dielectric constant to be a little smaller.²⁵ It is nearly certain also that point charges cannot adequately approximate the interionic interactions when hydronium ions are involved. It is useful, nevertheless, to determine approximate values of ϵ using our ΔH values of 3.2 ± 0.2 and 5.9 ± 0.4 kcal/mol plus the assumption of point charges and Coulomb's law.

We begin by making two estimates of the H⁺...O⁻ distance in the hydrogen bonds formed between the hydronium ions and the bisulfate ion.

Our first estimate involves the use of the bisulfate concentration measured by Raman spectroscopy for a 41.7 mol % sulfuric acid solution, namely, 13.6 M at 25 °C. From it we can obtain an average value for the interionic separation because the 42 mol % solution is a fused salt composed solely of the two types of hydronium-bisulfate ion pairs. The interionic distance calculated from $9.4c^{-1/3}$ ²⁰ is 3.94 Å. If we then consider that this interionic distance involves an S=O double bond (1.42 Å) plus the average O-H bond of the two types of hydronium ions (1.0 Å), then we obtain 1.52 Å for the H⁺...O⁻ distance.

Our second estimate employs X-ray data from the 50 mol % solid. We take the average of the O(5)···O(1) and O(5)···O(2) X-ray values,⁶ which is 2.552 Å, and subtract 1.02 Å, giving 1.53 Å for the H⁺...O⁻ distance.

The agreement, 1.52 Å versus 1.53 Å, is good. It buttresses Young's Raman-determined bisulfate ion concentration⁵ and our conclusion that the 42 mol % solution is a hydronium-bisulfate molten salt.

If we use the value of 1.53 Å from the X-ray data and assume point charges, we obtain $\epsilon = 67$ for $\Delta H = 3.2 \pm 0.2$ kcal/mol and $\epsilon = 36$ for $\Delta H = 5.9 \pm 0.4$ kcal/mol.

In view of the above ϵ values and because the H₃O⁺-HSO₄⁻ concentration is waning at 360 °C and the H₅O₂⁺-HSO₄⁻ concentration approaches zero near the critical point, we may expect that $\epsilon \approx 67$ at room temperature and decreases to roughly 36 in the vicinity of 360 °C. A further decrease (e.g., to between 1 and 10) probably occurs as the critical point, 665 °C, is approached. This additional decrease is likely because virtually all hydrogen bonds are broken and the system is composed almost exclusively of neutral molecules—H₂SO₄, H₂O, and SO₃—near 665 °C (and a pressure of 0.5 ± 0.1 kbar) (cf. $\epsilon = 2.7$ for water at 0.5 kbar and 550 °C).²⁶

Appendix

A plot of $Y = \ln[(D - CF)/C^2]$ versus $1/T$ is shown in Figure 19. The Raman data involve peak-height measurements at 905 and 1035 cm⁻¹ and correspond to the equilibrium constant $[H_2SO_4]/[HSO_4^-]^2$, which is proportional to $(D - CF)/C^2$ (the reciprocal of the form used by Young et al.⁵).

The slope shown in Figure 19 corresponds to a ΔH of 4400 cal/mol with $F = 0.4247$. This ΔH value is simply an overly large variant of the previous ΔH values that were obtained without squaring C . Moreover, the F value is also somewhat

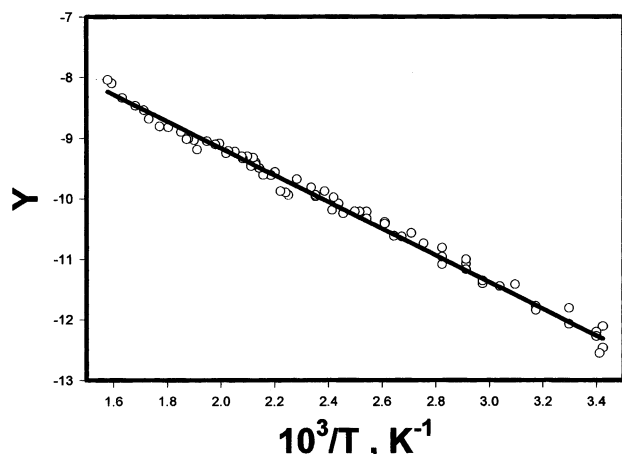


Figure 19. Plot of $Y = \ln[(D - CF)/C^2]$ versus $1/T$ for 42 mol % sulfuric acid 905/1035- cm^{-1} peak-height ratios. The heavy line represents the least-squares fit; $\Delta H = 4400$ cal/mol.

too large; see the peak-height F value of 0.412 ± 0.01 and the other F values in Table 2.

One might argue that $(D - CF)/C^2$ corresponds to the reaction $\text{H}^+ + \text{HSO}_4^-$ (ref 1) = H_2SO_4 .¹ However, the ΔH for this reaction is about -250 kcal/mol⁴ versus $+4.4$ kcal/mol that is observed here, providing clear evidence that the bare proton H^+ does not exist in sulfuric acid.

Davis, Adams, and McGuire²⁷ reported high-pressure Raman intensity data for the bisulfate/sulfate equilibrium, $\text{HSO}_4^- + \text{H}_2\text{O} = \text{H}_3\text{O}^+ + \text{SO}_4^{2-}$. The integrated Raman intensity ratio, $I_R = I(\text{SO}_4^{2-})/I(\text{HSO}_4^-)$, was measured versus pressure using the sulfate 980- cm^{-1} line and the HSO_4^- line at ~ 1035 cm^{-1} . Four isotherms from 281.15 to 300.65 K were examined, with pressures ranging from ~ 1 atm to 1029 bar.

The isothermal pressure rise was found to increase the sulfate ion concentration relative to the bisulfate ion concentration, but a quantitative explanation was not presented.

We subjected the data of Davis et al. to least-squares analysis. This allowed us to obtain the derivative $[\partial \ln I_R/\partial P]_T = -\Delta V/RT$ at each temperature. The corresponding ΔV values are -11.0 cm^3/mol (300.65 K), -12.0 cm^3/mol (291.65 K), -11.9 cm^3/mol (286.15 K), and -10.8 cm^3/mol (281.15 K), averaging -11.4 cm^3/mol .

This large negative volume change cannot be explained by the volume differences of unhydrated sulfate and bisulfate ions.

We calculated ΔV as follows. We assumed that the bisulfate ion is hydrogen bonded to four water molecules all having the normal asymmetric H-bond O—O distance of 2.84 Å. We next assumed that the hydronium—sulfate H-bond distance decreases to 2.54 Å following the transfer of the proton from the bisulfate ion to the water, which results in the formation of one hydrogen bond (out of the original four) approaching the symmetric distance. We assumed that the remaining three normal H-bonds retained their 2.84-Å distances.

Note that we are invoking a double-well potential of the same type as that used above for the first dissociation of sulfuric acid.

ΔV was calculated from $(4/3)\pi(R_1^3 - R_2^3)N_A$, where N_A is Avogadro's number and R_1 is the average radius of the hydrated sulfate ion, that is, the sulfate ion is H-bonded to three water molecules (O—O = 2.84 Å) and to one hydronium ion (O—O

= 2.54 Å). R_2 is the radius of the hydrated bisulfate ion when surrounded by four water molecules (O—O = 2.84 Å). We used 1.51 Å for all S—O distances.

Our calculated $\Delta V = -10.6$ cm^3/mol compared to the measured average value of -11.4 cm^3/mol . The agreement is $\sim 8\%$, which is quite satisfactory because it is almost within the uncertainty in the experimental value, $\Delta V = -11.4 \pm 0.5$ cm^3/mol , when the approximate nature of the calculation is considered.

The point of the above calculation is that the sulfate/bisulfate equilibrium is best explained by a double-well potential, in direct analogy to the double-well potential used for the bisulfate ion/sulfuric acid equilibrium. Sulfate ion hydrogen-bonded to the hydronium ion plus three water molecules refers to a low-volume, low-energy⁵ state, whereas bisulfate ion hydrogen bonded to four water molecules is in a high-volume, high-energy state relative to that of the sulfate ion.

References and Notes

- (1) Brønsted, J. N. *Z. Phys. Chem.* **1910**, *68*, 693.
- (2) Giauque, W. F.; Hornung, E. W.; Kunzler, J. E.; Rubin, T. F. *J. Am. Chem. Soc.* **1960**, *82*, 62.
- (3) The data of reference 1 as treated in Lewis, G. N.; Randall, M. *Thermodynamics and the Free Energy of Chemical Substances*; McGraw-Hill: New York, 1923; p 95, Table 7, were subjected to least-squares analysis using a seventh-degree polynomial. Data of reference 2 were subjected to least-squares analysis using a fifth-degree polynomial.
- (4) Walrafen, G. E.; Yang, W.-H.; Chu, Y. C.; Hokmabadi, M. S. *J. Solution Chem.* **2000**, *29*, 905.
- (5) Young, T. F.; Maranville, L. F.; Smith, H. M. In *The Structure of Electrolytic Solutions*; Hamer, W. J., Ed.; Wiley: New York, 1959.
- (6) Taesler, I.; Olovsson, I. *Acta Crystallogr., Sect. B* **1968**, *24*, 299.
- (7) Walrafen, G. E.; Abebe, M.; Mauer, F. A.; Block, S.; Piermarini, G. J.; Munro, R. *J. Chem. Phys.* **1982**, *77*, 2166.
- (8) Dawson, B. S. W.; Irish, D. E.; Togood, G. E. *J. Phys. Chem.* **1986**, *90*, 334.
- (9) Klotz, I. M.; Eckert, C. F. *J. Am. Chem. Soc.* **1942**, *64*, 1878. Young, T. F.; Singletary, C. R.; Klotz, I. M. *J. Phys. Chem.* **1978**, *82*, 671.
- (10) Walrafen, G. E.; Fisher, M. R.; Hokmabadi, M. S.; Yang, W.-H. *J. Chem. Phys.* **1986**, *85*, 6970.
- (11) Walrafen, G. E. In *Hydrogen-Bonded Liquids*; Dore, J. C., Teixeira, J., Eds.; Kluwer Academic: Dordrecht, The Netherlands, 1990.
- (12) Walrafen, G. E. *J. Phys. Chem.* **1990**, *94*, 2237.
- (13) Stuckey, J. E.; Secoy, C. H. *J. Chem. Eng. Data* **1963**, *8*, 386.
- (14) Catti, M.; Ferraris, G.; Ivaldi, G. *Acta Crystallogr., Sect. B* **1979**, *35*, 525.
- (15) Lau, Y. K.; Ikuta, S.; Kebarle, P. *J. Am. Chem. Soc.* **1982**, *104*, 1462.
- (16) Walrafen, G. E.; Yang, W.-H.; Chu, Y. C. *J. Phys. Chem. B* **2001**, *105*, 7155.
- (17) Considerable effort has been expended (Walrafen) in an attempt to find Raman evidence for charged species in, and above, various acid solutions at very high temperatures, but with negative results. This failure may be related to the fact that the attractive forces between oppositely charged ions are strong when the dielectric constant is low.
- (18) Vermeulen, T. In *Perry's Chemical Engineers' Handbook*, 7th ed.; Perry, R. H., Ed.; McGraw-Hill: New York, 1997.
- (19) Walrafen, G. E. *J. Chem. Phys.* **1964**, *40*, 2326.
- (20) Robinson, R. A.; Stokes, R. H. *Electrolyte Solutions*; Butterworths: London, 1959; p 5.
- (21) Newton, M. D.; Ehrenson, S. *J. Am. Chem. Soc.* **1971**, *93*, 4971.
- (22) Ratcliff, C. I.; Irish, D. E. In *Water Science Reviews*; Franks, F., Ed.; Cambridge University Press: Cambridge, U.K., 1961; p 161.
- (23) Walrafen, G. E.; Chu, Y. C. *J. Phys. Chem.* **1991**, *95*, 8909.
- (24) Hall, R. F.; Cole, R. H. *J. Phys. Chem.* **1981**, *85*, 1065.
- (25) Schellman, J. A. *J. Chem. Phys.* **1957**, *26*, 1225.
- (26) Tödheide, K. In *The Physics and Physical Chemistry of Water*; Water: A Comprehensive Treatise; Franks, F., Ed.; Plenum Press: New York, 1972; Vol. 1.
- (27) Davis, A. R.; Adams, W. A.; McGuire, M. J. *J. Chem. Phys.* **1974**, *60*, 1751.